ANALYTICAL METHOD FOR ESTIMATION ISOTOPE YIELD UNDER PHOTONUCLEAR PRODUCTION

V.I. Nikiforov, V.L. Uvarov
National Science Center "Kharkov Institute of Physics and Technology", Kharkov, Ukraine
E-mail: uvarov@kipt.kharkov.ua

The heuristic model for description space-energy characteristics of the high-energy bremsstrahlung has been developed. On its basis the method for analytical estimation photonuclear yield of isotopes in wide range of atomic number (Z=20-80) and size of a target as well as of the electron energy (40…100 MeV) is proposed. The analysis of validity of the model assumptions has been executed by means of it comparison with the results of simulation using the program package PENELOPE/2006 [1] supplemented with database on the cross-sections of photonuclear reactions. It has been shown earlier that such simulation method provides close fit with the experimental results. As an example the reactions of practical interest ^{48}Ti(γ,p)^{47}Sc, ^{68}Zn(γ,p)^{67}Cu and ^{187}Re(γ,n)^{186}Re are presented.

PACS: 07.85.-m, 81.40wx, 87.53-j, 87.53.Wz

1. INTRODUCTION

1.1. In the general case, the output devices of the electron linac operated in the mode of isotope production include a converter C in the form of a *d* thick plate made from the material with great Z, and a target T in the form of a cylinder of radius R and height H, which is axially symmetric about the beam (see Fig.1). As a result of the interaction between accelerated electrons and the converter, a flux of bremsstrahlung photons (or X-ray) escapes from the converter. The photon energy ω is continuously distributed in the spectrum in the range $0 < \omega \le \omega_{max}=E_0$. Simultaneously, a flux of electrons escapes from the converter. Their number and spectral distribution being determined by the E_0 value, and also, by the converter material and thickness. Thus, a flux of mixed e,X-radiation is formed in the converter and the target, which is responsible for thermophysical and radiation conditions of these devices [2].

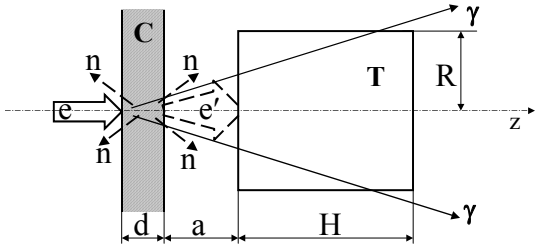

Fig.1. Arrangement of basic elements for photonuclear production of isotopes

In addition, as a result of (γ,n) reactions occurring in the converter, a quasi-isotropic photoneutron flux escapes from the converter. As an example of these reactions that occur in the natural tungsten converter we mention the ^{182}W(γ,n)^{181}W and ^{186}W(γ,n)^{185}W reactions. The photoneutrons may also initiate the yield of different isotopes in the target [3]. In the context of the given problem, we restrict ourselves to the consideration of (γ,N) reactions only, because (γ,2n), (γ,np), (γ,α), (e,e'), (n,γ) and other channels generally have substantially lower cross section values.

1.2. The processes of high-energy photon transfer in material media are generally described with the use of the attenuation coefficient μ(Z,ω) [4]. In particular, the intensity of the "narrow" photon beam dies away in the target depth in proportion to exp[-μ(Z,ω)·z]. The μ^{-1} value characterizes the so-called "free path" of photons. So, strictly speaking, the reactions with photon participation can occur in the whole half-space behind the converter (R→∞, H→∞). With an increasing target size the total yield of the isotope product in the *i*-type reaction (normalized to one accelerated electron) tends to its theoretical limit $y_i^{\infty}(E_0)$. As an example, Fig.2 shows the simulated distribution of ^{47}Sc nuclei that are produced in a large titanium target (R=10 cm, H=15 cm) under the action of bremsstrahlung.

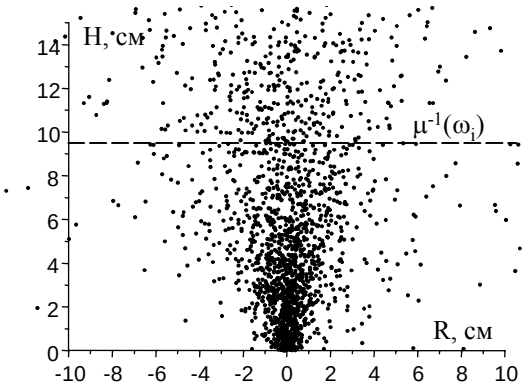

Fig.2. Distribution of ^{47}Sc nuclei in the Ti target (E_0=100 MeV)

Thus, at the initial stage of developing the photonuclear technology, the main task consists in estimating the isotope yield for real parameters of the accelerator (electron energy E_0, the average beam current I and beam size), and also, in optimizing the target dimensions (R, H) with regard to the total and specific activity. The key parameters of the problem are as follows:

- electron beam density distribution on the converter;
- converter's material and thickness d;
- value of gap a between the converter and the target.

1.3. The number of new nuclei in the target per one accelerated electron can be described in the general case by the following formula:

$$y_i = \nu_T \cdot \rho_T \frac{N_A}{\bar{A}} \int_V dV \int_{\omega_{i,th}}^{E_0} \dot{\Phi}_\gamma(\vec{r},\omega)\sigma_i(\omega)d\omega, \qquad (1)$$

where $\dot{\Phi}_\gamma(\vec{r},\omega)$ is the differential fluence of bremsstrahlung photons of energy ω that are generated by a single electron in the target volume element having the radius-vector $\vec{r}$; $\sigma_i(\omega)$ – *i*-reaction cross section; $\omega_{i,th}$ – *i*-reaction energy threshold; ν_T – relative concentration of isotope-target nuclei; n_T – bulk concentration of nuclei in the target; V – target volume.

Thus, the problem reduces to analytic representation of the functions $\dot{\Phi}_\gamma(\vec{r},\omega)$, $\sigma_i(\omega)$ and to calculation of integral (1). From its form it follows, in particular, that in our calculations it will be sufficient to take into account only the high-energy part of the photon spectrum $\omega_{i,th}=\omega_{min}\le\omega\le E_0$. Those photons will be referred to as "effective".

2. DESCRIPTION OF BREMSSTRAHLUNG

2.1. PHOTON ENERGY DISTRIBUTION

It follows from the simulation data that the dependence of the spectral bremsstrahlung intensity on photon energy ω for a thick converter can be described in the linear approximation by the following expression

$$\omega\frac{\partial N_\gamma(E_0,d,\omega)}{\partial\omega}\approx b-c\omega. \qquad (2)$$

By extending this approximation to the whole photon energy range $0<\omega\le E_0$, it appears possible to determine the coefficients *b* and *c* from the conditions

$$\left.\frac{\partial N_\gamma}{\partial\omega}\right|_{\omega=E_0}=0, \qquad (2.1)$$

$$\int_0^{E_0}\omega\frac{\partial N_\gamma}{\partial\omega}d\omega=\eta(E_0,d)E_0, \qquad (2.2)$$

where η is the conversion coefficient. This coefficient is defined as the ratio of the total energy of bremsstrahlung photons to the primary electron energy.

Thus, in the linear approximation, we can obtain the following expressions for the spectral photon distribution in the $0<\omega\le E_0$ range

$$\frac{\partial N_{\gamma,1}}{\partial\omega}(E_0,d,\omega)=2\eta(E_0,d)\left(\frac{1}{\omega}-\frac{1}{E_0}\right), \qquad (3)$$

and also, for the "effective" photon yield ($\omega_{min}<\omega\le E_0$)

$$\Delta N_{\gamma,1}(E_0,d,\omega_{min})=2\eta(E_0,d)\cdot\left[\frac{\omega_{min}}{E_0}-\ln\left(\frac{\omega_{min}}{E_0}\right)-1\right]. \qquad (4)$$

Formula (4) provides the estimation of the "effective" photon yield from the conversion coefficient value. The last one can be determined experimentally with the use of a thick-wall ionization chamber or a calorimeter or by the simulation technique. So, Fig.3 shows the conversion coefficient as a function of the W converter thickness, and Table 1 lists the ΔN_γ values for different reactions, calculated by formula (4) and obtained by the simulation technique (ω_{min}=7.2 MeV corresponds to the $^{186}W(\gamma,n)^{185}W$ reaction threshold, being the lowest from among those considered in the present work). From the data presented in Fig.3 it follows that in the 40…100 MeV range the maximum conversion coefficient value is within the limits of 0.42…0.51.

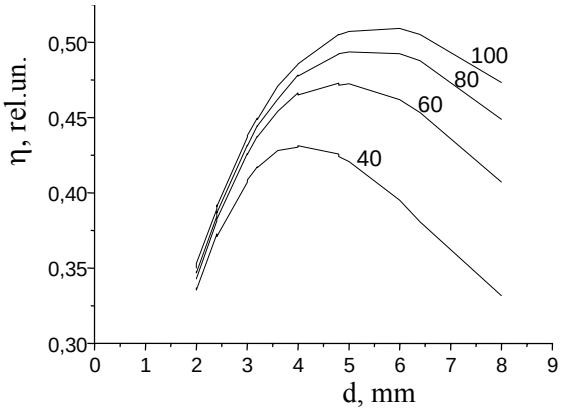

Fig.3. Energy conversion coefficient versus W converter thickness. The figures indicate the electron energy E_0 in MeV units

Table 1

"Effective" photon yields for different reactions (W converter, d=4 mm)

E_0, MeV / Reaction	40		60		80		100	
	ΔNγ1	ΔNγ	ΔNγ1	ΔNγ	ΔNγ1	ΔNγ	ΔNγ1	ΔNγ
$^{48}Ti(\gamma,p)^{47}Sc$	0.4527	0.3772	0.7782	0.6895	1.027	0.9430	1.230	1.1572
$^{68}Zn(\gamma,p)^{67}Cu$	0.5482	0.4693	0.8945	0.8118	1.153	1.0831	1.362	1.3093
$^{187}Re(\gamma,n)^{186}Re$	0.7526	0.6813	1.136	1.0818	1.411	1.3884	1.631	1.6403

The analysis of the data in Table 1 shows that the linear approximation of the bremsstrahlung spectrum gives an overestimated value of the "effective" photon yield (up to 20%) at the lower boundary of the Z and E_0 value ranges under consideration. At the same time, the divergence practically disappears at the upper boundary of the mentioned ranges. This is due to a certain radiant energy redistribution between the lower and middle parts of the spectrum at its linear approximation.

2.2. SPACE-ANGULAR DISTRIBUTION OF PHOTONS

The peculiarity of electron dynamics in the linear accelerator lies in the limitation of the cross-sectional size of the beam by the aperture of the accelerating structure along the whole path of beam formation. Therefore, the angular divergence of electrons on the front surface of the converter can be neglected. The probability density function of their radial distribution is commonly described by the Gaussian law [5]

$$\frac{dP_e}{dS}=\frac{1}{2\pi\delta_e^2}\exp\left(-\frac{r^2}{2\delta_e^2}\right), \qquad (5)$$

where δ_e is the standard deviation of the distribution.

The generation of bremsstrahlung photons and the angle of their escape from the converter are determined by the processes of accelerated-electron multiple scattering in the converter. Therefore, we shall assume that

the radial and angular photon distributions behind the converter can also be described by the Gaussian distribution with the standard deviations $\delta_{\gamma,r}(E_0,d)$ and $\delta_{\gamma,\theta}(E_0,d)$, respectively.

The simulation method was used to calculate the radial and angular distributions of "effective" photons (ω_{min}=7.2 MeV) for the W converter of different thickness at various E_0 values. The distributions were approximated by the Gaussian functions with the result that the following standard deviation $\delta_{\gamma,r}$ as functions of the converter thickness d ranging from 0 to 1 cm was obtained:

$$\delta_{\gamma,r}(d) = \delta_e + k(E_0)\cdot d^{3/2}. \quad (6)$$

For the 0.4 cm thick W converter the coefficient $k(E_0)$ value is variable from 0.053 (E_0 = 40 MeV) to 0.029 (E_0 = 100 MeV).

As an estimate of the average exit angle of "effective" photons from the converter $\bar{\theta}(E_0,d)$, we take

$$\bar{\theta}(E_0,d) = \sqrt{2\ln 2}\,\delta_{\gamma,\theta}(E_0,d) \approx 1.177\,\delta_{\gamma,\theta}(E_0,d), \quad (7)$$

which corresponds to the half-width at half-height of the θ distribution. From simulation results it follows that for the 0.4 cm thick converter the θ value lies within the range from 7.2° (E_0=40 MeV) to 3.8° (E_0=100 MeV). So, the standard deviation of the radial photon flux distribution behind the converter in the plane with the coordinate z (z = 0 corresponds to the front surface of the converter) is given by

$$\delta_{\gamma,r}(E_0,d,z) = \delta_e + k(E_0)\cdot d^{3/2} + (z-d)\cdot tg\bar{\theta}(E_0,d). \quad (8)$$

Henceforth, to take into account the photon flux density variation along the target axis owing to the angular divergence of the flux, we shall use the $\delta_{\gamma,r}$ value at the target half-height or at $z = d + a + H/2$.

3. THE PHOTONUCLEAR YIELD OF ISOTOPES IN THE CYLINDRICAL TARGET

3.1. To express analytically the photonuclear reaction cross section $\sigma_i(\omega)$, we make use of the customary form of description of the giant dipole resonance [6]:

$$\sigma_i(\omega) = \sigma_i^{max}\cdot\frac{(\omega\Gamma_i)^2}{(\omega^2-\omega_i^2)^2+(\omega\Gamma_i)^2}, \quad (9)$$

where Γ_i is the excitation function width at half-height, ω_i is the photon energy corresponding to the cross section peak σ_i^{max}.

Table 2 gives the characteristics of both the cross sections for the reactions under consideration and the target material of natural isotopic composition.

Table 2

Parameters of target materials and excitation functions

Reaction	ρ_T, г/cm^3	ν_T	ω_i^{th}, MeV	σ_i^{max}, mb	ω_i, MeV	Γ_i, MeV
^{48}Ti(γ,p)^{47}Sc	4.54	0.738	11.6	6.8	21.3	7.32
^{68}Zn(γ,p)^{67}Cu	7.133	0.188	9.99	10.76	23.16	8.82
^{187}Re(γ,n)^{186}Re	21.02	0.626	7.38	424.65	13.19	3.67

3.2. For the case of the cylindrical target axially symmetric with radiant flux formula (1) can be rewritten as

$$y_i(E_0) = \nu_T\rho_T\frac{N_A}{\bar{A}}\int_{d+a}^{d+a+H}dz\int_0^R 2\pi r dr\int_{\omega_{th}}^{E_0}\dot{\Phi}_\gamma(z,r,\omega)\cdot\sigma_i(\omega)d\omega. \quad (10)$$

At linear approximation of the spectrum (3), the expression for the normalized differential fluence of "effective" photons with allowance made for attenuation of their flux in the target material can be represented as

$$\dot{O}_{\gamma,1}(z,r,\omega) = \frac{\eta(E_0,d)}{\pi\delta_{\gamma,r}^2(z)}\left(\frac{1}{\omega}-\frac{1}{E_0}\right)\cdot\exp\left\{-\left[\frac{r^2}{2\delta_{\gamma,r}^2(z)}+\mu(\omega)\cdot(z-d-a)\right]\right\}, \quad (11)$$

where $\delta_{\gamma,r}(z)$ is determined by formula (6).

3.3. According to the simulation results, in the 10≤ω≤50 MeV range overlapping the giant dipole resonance region, the photon attenuation coefficient $\mu(\omega)$ varies only very slightly practically for all the materials. Taking also into account the form of the excitation function $\sigma_i(\omega)$, in the further calculations we can put $\mu(\omega)=\mu(\omega_i)$. Then, substituting eq. (9), (11) into formula (10) and integrating over r and z we obtain

$$y_i = 2\nu_T\cdot\rho_T\frac{\eta(E_0,d)\cdot\sigma_i^{max}\cdot N_A}{\bar{A}}\left[1-\exp\left(-\frac{R^2}{2\delta_{\gamma,r}^2(d+a+H/2)}\right)\right]\cdot$$
$$\cdot\frac{1-\exp[-\mu(\omega_i)\cdot H]}{\mu(\omega_i)}\cdot S_{i,1}(E_0), \quad (12)$$

where

$$S_{i,1}(E_0) = \int_{\omega_{i,th}}^{E_0}\frac{(\omega\Gamma_i)^2}{(\omega^2-\omega_i^2)^2+(\omega\Gamma_i)^2}\cdot\left(1-\frac{\omega}{E_0}\right)\cdot\frac{d\omega}{\omega}. \quad (13)$$

After replacement of the variables

$$\varepsilon = \frac{\omega}{\Gamma_i},\ \varepsilon_i = \frac{\omega_i}{\Gamma_i},\ \varepsilon_0 = \frac{E_0}{\Gamma_i},\ \varepsilon_{i,th} = \frac{\omega_{i,th}}{\Gamma_i}, \quad (14)$$

formula(13) takes on the form

$$S_{i,1}(E_0) = \int_{\varepsilon_{i,th}}^{\varepsilon_0}\frac{\varepsilon}{(\varepsilon^2-\varepsilon_i^2)^2+\varepsilon^2}\cdot\left(1-\frac{\varepsilon}{\varepsilon_0}\right)d\varepsilon =$$
$$= \left[\Psi(\varepsilon_0)-\Psi(\varepsilon_{i,th})\right], \quad (15)$$

where

$$\Psi(\varepsilon) = \Psi_1(\varepsilon)-\frac{1}{2\varepsilon_0 D}\left[\Psi_2^-(\varepsilon)-\Psi_2^+(\varepsilon)\right], \quad (16)$$

$$\Psi_1(\varepsilon) = \frac{1}{D}arctg\left[\frac{2(\varepsilon^2-\varepsilon_i^2)+1}{D}\right], \quad (17)$$

$$\Psi_2^{\pm}(\varepsilon) = \frac{1}{2}\ln(\varepsilon^2\pm D\varepsilon+\varepsilon_i^2)\mp D\cdot arctg(2\varepsilon\pm D),$$
$$D = \sqrt{4\varepsilon_i^2-1}. \quad (18)$$

Finally, the expression for the normalized yield of isotopes in the cylindrical target can be represented in the following form

$$y_i(E_0) = \left\{1-\exp\left[-\frac{R^2}{2\delta_{\gamma,r}^2(d+a+H/2)}\right]\right\}\cdot$$
$$\cdot\left\{1-\exp[-\mu(\omega_i)\cdot H]\right\}\cdot y_i^{\infty}(E_0), \quad (19)$$

where the yield in the semi-infinite target is given by

$$y_i^{\infty}(E_0) = 2\nu_T\rho_T\frac{N_A}{\bar{A}}\cdot\sigma_i^{max}\cdot\frac{\eta(E_0,d)}{\mu(\omega_i)}\cdot[\Psi(\varepsilon_0)-\Psi(\varepsilon_{i,th})]. \quad (20)$$

3.4. The maximum volume velocity of isotope product generation falls on the front surface of the target in the neighborhood of the target axis (z=d+a; r=0), where

the photon flux density is the highest. For this region, the normalized specific yield of the isotope can be determined as

$$y_i^{\max} = \left(\frac{dy_i}{dm_T}\right)^{\max} = \nu_T \frac{N_A}{A} \frac{\eta(E_0, t_c)}{\pi \delta_{\gamma,r}^2 (d+a)} \sigma_i^{\max} \cdot$$

$$\cdot [\Psi(\varepsilon_0) - \Psi(\varepsilon_{i,th})]. \qquad (21)$$

3.5. With formulas (19)-(21) it is easy to estimate the total activity of the target and its peak specific activity after the time of exposure τ at an average electron beam current I as

$$A_i(\tau) = \frac{I \cdot y_i(E_0)}{e} \left[1 - \exp\left(-\frac{\ln 2}{T_i} \cdot \tau\right)\right], \qquad (22)$$

where e is the electron charge, T_i is the half-life of the isotope.

3.6. Figs.4 to 6 show the normalized photonuclear yields of ^{47}Sc, ^{67}Cu and ^{186}Re isotopes as functions of the electron energy E_0 (δ_e=0.25 cm; d=0.4 cm) for the targets from natural materials, measuring 2RxH (cm).

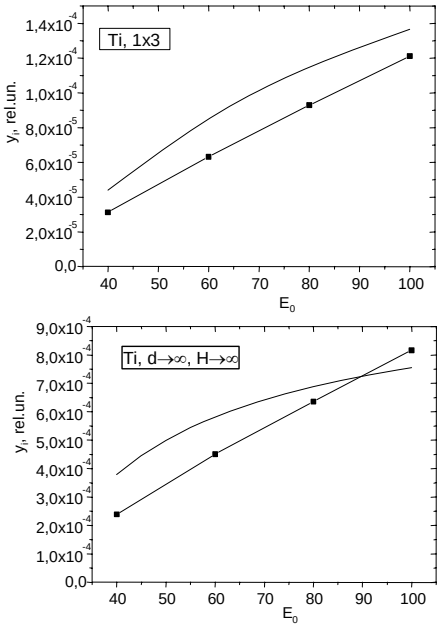

Fig.4. Sc-47 yield from the Ti target

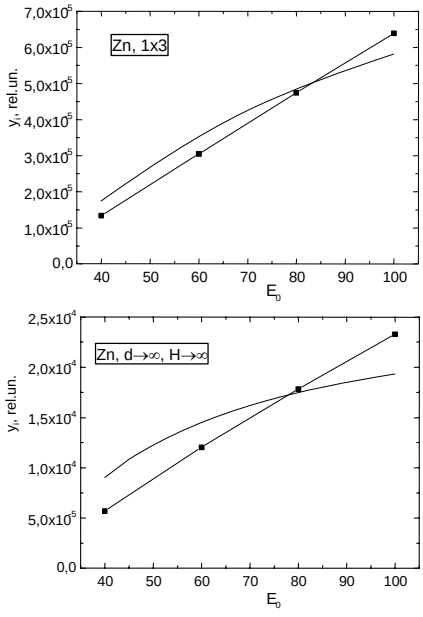

Fig.5. Cu-67 yield from the Zn target

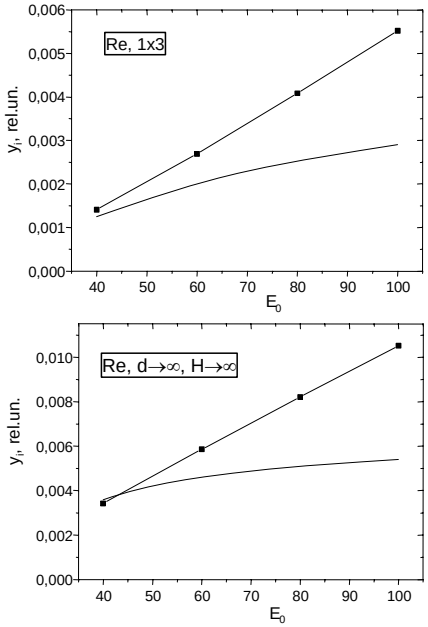

Fig.6. Re-186 yield from the Re target

The data were obtained through calculations by formulas (19), (20), and also through simulation with due regard for the excitation functions measured experimentally [6]. The last ones are denoted in the figures by the ■ symbol. The $[\Psi(\varepsilon_0) - \Psi(\varepsilon_{i,th})]$ function values for the reactions are listed in Table 3.

Table 3

The $[\Psi(\varepsilon_0) - \Psi(\varepsilon_{i,th})]$ *function values*

E_0, MeV / Reaction	40	60	80	100
^{48}Ti(γ,p)^{47}Sc	0.1995	0.2829	0.3265	0.3532
^{68}Zn(γ,p)^{67}Cu	0.2026	0.3011	0.3532	0.3853
^{187}Re(γ,n)^{186}Re	0.2474	0.2922	0.3150	0.3288

CONCLUSIONS

The high-energy bremsstrahlung flux, to which the processing target is exposed, is substantially inhomogeneous. The radiation intensity and its distribution in the target volume are governed not only by the electron energy and the average beam current, but also by the beam size, the converter thickness and material, as well as by the target size and location. As a rule, the target interacts only with a part of the photon flux, and as a result, an uncertainty arises between the target activity and the electron beam charge. It is just here lies the vital difference between photoactivation and the heavy particle activation, when practically the whole beam charge is localized in the target. Therefore, the normalization of the isotope yield to the beam charge (accepted in accelerator technologies) without a detailed description of activation conditions, appears not quite correct, as applied to the photonuclear method.

The analysis of the data in Figs. 4 to 6 shows that the proposed model gives overestimated isotope yield values for the targets with Z<30. The discrepancy decreases till the coincidence of the results is attained in the region of Z ≈ 40, E_0 ≈ 50 MeV. With an increase in the electron energy the model starts to give underesti-

mated yield values. The discrepancy becomes greater at $Z \rightarrow 80$ (see Fig.6).

The mentioned difference between the analytical estimation data and the simulation data can be explained by the fact that the proposed approximation of the bremsstrahlung spectrum (see formula (3)) gives overestimated (up to 20%) "effective" photon yield values for all the reactions at $E_0 < 100$ MeV, the discrepancy decreasing with an increase in Z and E_0 (see Table 1). The reversal of the sign of discrepancy between the isotope yield data in the region of $Z>40$, $E_0>50$ is due to the fact that the proposed model takes into account the channel of isotope production only under the action of photons generated in the converter. At the same time, as the Z value of the target and the electron energy increase, there grows the contribution from the reactions due to photons produced in the target itself by the high-energy part of the electron flux that has passed through the converter.

REFERENCES

1. F. Solvat, J.M. Fernandez-Varea, I. Sempau. *PENELOPE-2006 a Code System for Monte-Carlo Simulation of Electron and Photon Transport*. OECD Nucl. Ener. Agency (Issyles – Moulineous) France. 2006.
2. V.I.Nikiforov, V.L.Uvarov. Analysis of Mixed e,X Radiation along the Extraction Facilities of Electron Accelerators // *Atomic Energy*. 2009, v.106, №4, p.220-224.
3. N.P. Dikiy, A.N. Dovbnya, V.L. Uvarov. Electron Accelerator Based Soft Technology for Medical Imaging Isotopes Production // *Proc. 8-th Europ. Part. Accel. Conf. EPAC'02. Paris (France), June 3-7,* 2002, p.2760-2762.
4. I.H. Hubbel. Photon Mass Attenuation and Energy-absorption Coefficients from 1 keV to 20 MeV *// Int. J. Appl. Rad. Isot*. 1982, v.33, №12, p.1269-1290.
5. Radiation Dosimetry: Electron Beams with Energies between 1 and 50 MeV // *ICRU Report* 35, 1984.
6. Handbook on photonuclear data for Applications // *Final report of coordinated researched projects.* IAEA. TECDOC. Draft N 3 (Culham). 11 February 2000.

Статья поступила в редакцию 02.12.2009 г.

АНАЛИТИЧЕСКИЙ МЕТОД ОЦЕНКИ ВЫХОДА ИЗОТОПОВ ПРИ ФОТОЯДЕРНОМ ПРОИЗВОДСТВЕ

В.И. Никифоров, В.Л. Уваров

Разработана эвристическая модель для описания пространственно-энергетических характеристик высокоэнергетичного тормозного излучения. Предложен метод с ее использованием для аналитической оценки фотоядерного выхода изотопов в широком диапазоне значений атомного номера (Z=20-80) и размеров мишени, а также энергии электронов (40…100 МэВ). Проведен анализ обоснованности допущений модели путем ее сопоставления с результатами моделирования на основе программной системы PENELOPE/2006, дополненной базой данных по сечениям фотоядерных реакций. Ранее было показано, что такой метод моделирования дает хорошее согласие с результатами эксперимента. В качестве примера рассмотрены представляющие практический интерес реакции $^{48}Ti(\gamma,p)^{47}Sc$, $^{68}Zn(\gamma,p)^{67}Cu$ и $^{187}Re(\gamma,n)^{186}Re$.

АНАЛІТИЧНИЙ МЕТОД ОЦІНКИ ВИХОДУ ІЗОТОПІВ ПРИ ФОТОЯДЕРНОМУ ВИРОБНИЦТВІ

В.І. Нікіфоров, В.Л. Уваров

Розроблено евристичну модель для опису просторово-енергетичних характеристик високоенергетичного гальмівного випромінювання. Запропоновано метод з її використанням для аналітичної оцінки фотоядерного виходу ізотопів у широкому діапазоні значень атомного номера (Z=20-80) і розмірів мішені, а також енергії електронів (40…100 МеВ). Проведено аналіз обгрунтованості припущень моделі шляхом її порівнювання з результатами моделювання на основі програмної системи PENELOPE/2006, доповненої базою даних з перетинів фотоядерних реакцій. Раніше було показано, що такий метод моделювання дає добре погодження з результатами експерименту. Як приклад розглянуто реакції $^{48}Ti(\gamma,p)^{47}Sc$, $^{68}Zn(\gamma,p)^{67}Cu$ і $^{187}Re(\gamma,n)^{186}Re$, що мають практичний інтерес.